


Cite this: *RSC Adv.*, 2020, 10, 13021

Direct electrochemical detection of clozapine by RuO₂ nanoparticles-modified screen-printed electrode

Mohammad Reza Aflatoonian,^{ab} Somayeh Tajik,^{*ac} Bita Mohtat,^d Behnaz Aflatoonian,^a Iran Sheikh Shoaie,^{id e} Hadi Beitollahi,^{id f} Kaiqiang Zhang,^g Ho Won Jang^{id *g} and Mohammadreza Shokouhimehr^{id *g}

This study introduces the sensitive electrochemical detection of clozapine with the use of a ruthenium(IV) oxide nanoparticle (RuO₂ NP)-modified screen-printed electrode (RuO₂ NPs/SPE). The electrochemical behaviors of clozapine at RuO₂ NP/SPE have been examined *via* cyclic voltammetry (CV), differential pulse voltammetry (DPV) and chronoamperometry (CHA). According to the results, the modified electrode has been accompanied by a decreasing over-potential (*ca.* 170 mV) and enhancement in the peak current (3 times) in comparison with the bare SPE. The results indicated that RuO₂ NP/SPE markedly augmented electro-catalytic activities toward clozapine oxidation. In addition, linear responses have been observed in the range between 0.2 and 500.0 μM with a sensitivity of 0.076 $\mu\text{A } \mu\text{M}^{-1}$ and a limitation of detection of 0.07 μM (3σ). Moreover, the successful application of RuO₂ NP/SPE has been seen in detecting clozapine in real samples, which showed satisfied recoveries. Therefore, outputs suggest that RuO₂ NP/SPE will be promising for functional utilization.

Received 25th January 2020

Accepted 16th March 2020

DOI: 10.1039/d0ra00778a

rsc.li/rsc-advances

Introduction

According to the studies, schizophrenia is one of the serious chronic weakening diseases described by positive signs, such as hallucination and delusions, negative signs such as a socially withdrawn behavior and flat emotional expression, and cognitive deficiencies.¹ However, upon the introduction of clozapine (8-chloro-11-(4'-methyl-1 piperazinyl)-5H-dibenzo[*b,e*]-[1,4]-diazepine) that is the parent medicine of the so-called "typical" anti-psychotics, schizophrenia therapy experienced a good advancement. Clozapine is used to treat the negative and positive signs of patients with schizophrenia who do not respond well to the common neuroleptic medicines. Intoxication was evident at a high serum level of clozapine of 1158 ng mL⁻¹ during a trial with a dose of 800 mg d⁻¹.²

With regard to its significance, researchers utilized multiple techniques to detect clozapine in the drug and clinical preparations. The techniques consist of spectrophotometry,³ capillary zone electrophoresis,⁴ liquid chromatography-mass spectrometry,⁵ gas chromatography-mass spectrometry,⁶ high-performance liquid chromatography (HPLC),⁷ liquid chromatography-tandem mass spectrometry⁸ and electrochemistry.⁹⁻¹¹

Researchers further explored the electrochemical procedures because of benefits such as quicker responses, inexpensive instruments, easy preparation, cost-effectiveness, higher sensitivity, and good selectivity and stability.¹²⁻¹⁸

In addition, the screen-printed electrodes (SPEs) enjoy highly available and disposable electrochemical sensors, simplified operations and have non-poisonous features. Moreover, replacing traditional electrochemical cells with the SPEs linked to miniaturized potentiostats is one of the major trends in shifting the laboratory electrochemical instrumentations to the hand-held field analyzers. Furthermore, these electrodes are appropriate for operations with micro volumes and decentralized assays (point of care tests), and so forth.¹⁹⁻²³

To minimize the oxidation over-potential of numerous electroactive compounds, researchers designed the electro-catalytic procedures for exploitation at the modified electrode surface. Notably, the chemically modified electrodes augment the transfer rate of electrons by declining the over-potential.²⁴⁻³³

Nanoparticle (NP)-based CMEs have been the spotlight because of their increased sensitivity, amplified response signals, and more acceptable reproducibility.³⁴⁻⁴⁴

^aNeuroscience Research Center, Kerman University of Medical Sciences, Kerman, Iran

^bLeishmaniasis Research Center, Kerman University of Medical Sciences, Kerman, Iran. E-mail: tajik-s1365@yahoo.com

^cResearch Center for Tropical and Infectious Diseases, Kerman University of Medical Sciences, Kerman, Iran

^dDepartment of Chemistry, Karaj Branch, Islamic Azad University, Karaj, Iran

^eDepartment of Chemistry, Faculty of Science, Shahid Bahonar University of Kerman, Kerman 76175-133, Iran

^fEnvironment Department, Institute of Science and High Technology and Environmental Sciences, Graduate University of Advanced Technology, Kerman, Iran

^gDepartment of Materials Science and Engineering, Research Institute of Advanced Materials, Seoul National University, Seoul 08826, Republic of Korea. E-mail: hwjang@snu.ac.kr; mrsh2@snu.ac.kr

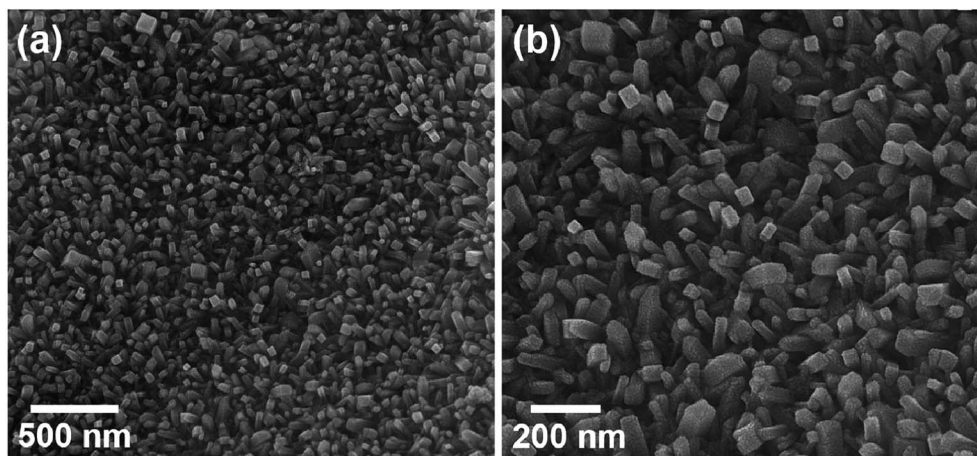



Fig. 1 SEM images of the as-synthesized RuO₂NPs.

In addition, ruthenium oxide (RuO₂) NPs have high potential as one of the electrochemical elements of sensors because of the respective attractive benefits; for example, acceptable electronic conductivity, very good catalytic capability, and higher chemical stability.^{45,46}

Accordingly, this study aimed at developing a RuO₂ NR/SPE, lowering the clozapine oxidation potential for its detection with no considerable effects from the background current. Thus, the study prepared an electrochemical sensor achieved by the modification of SPE by RuO₂ NPs and its application in detecting clozapine in the real specimens.

Experimental section

Reagents and instrument

We conducted electrochemical tests using an Autolab potentiostat/galvanostat (PGSTAT 302N, Eco Chemie: the Netherlands); then, we monitored the system by a general-purpose electrochemical system software.

It should be noted that SPE (DropSens: DRP-110, Spain) has 3 traditional electrodes called the graphite counter electrode, unmodified graphite working electrode, and a silver pseudo-reference electrode. Moreover, we used a Metrohm 710 pH-

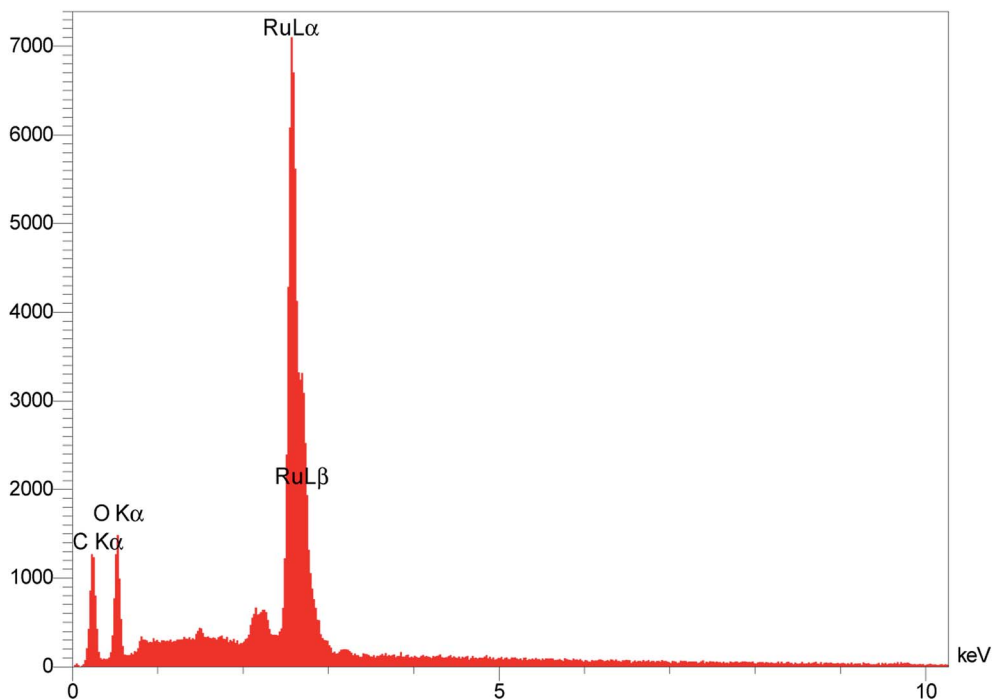


Fig. 2 EDX spectrum of RuO₂ NPs.



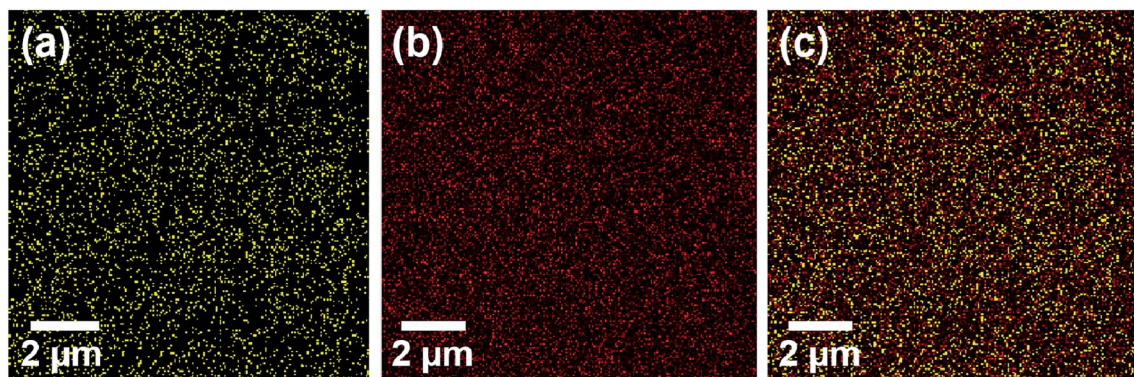


Fig. 3 EDX elemental mapping of the (a) O, (b) Ru, and (c) RuO₂.

meter for measuring pH. Milli-Q® IQ7003/05/10/15 water purification systems were used for preparing deionized water.

Clozapine and all the available reagents were of analytical grade. We chose Merck (Darmstadt: Germany) for purchasing the reagents. Thus, in order to procure the buffers, we applied *ortho*-phosphoric acid (85%) and respective salts for setting pH ranges between 2.0 and 9.0.

RuO₂ NP synthesis

According to the research design, 80 mL of water and 0.8 g of starch were blended and placed in a 60 °C water bath in order to gain a transparent solution. In addition, 1.2×10^{-2} mol of ruthenium chloride salt (99.9%) was added to the above solution. Then, pH was adjusted to 10.0 with a 1.0 M of ammonia solution. Consequently, the solution color changed to be black. Next, the solution was shaken for two hours and filtered. Finally, deionized water was used to wash it; therefore, when a thorough withdrawal of chlorine was ensured, the precipitate was dried and calcined at 450 °C for two hours.

Preparing the electrode

Based on the facile process presented below, the bare SPE was coated. Then, 1 mg of RuO₂ NPs were distributed in a 1 mL of aqueous solution over a 45 min ultra-sonication interval. Afterward, 5 μL of the procured suspension was dropped onto the carbon working electrode surface. Finally, it was left at room temperature in order to be dried.

Preparing the real samples

Clozapine tablets (Tehran Chemie Pharmaceutical Co., Iran [labelled value clozapine = 100 mg per tablet]) were purchased. The clozapine pills were thoroughly powdered and homogenized prior to the preparation of 10 mL of a 0.1 M stock solution. In fact, we sonicated the solution for assuring an ideal dissolution. Then, we filtered the solution. Furthermore, we poured the determined volume of the transparent filtrate into an electrochemical cell consisting of 10 mL of 0.1 M PBS (pH 7.0) for recording the differential pulse voltammetry (DPV).

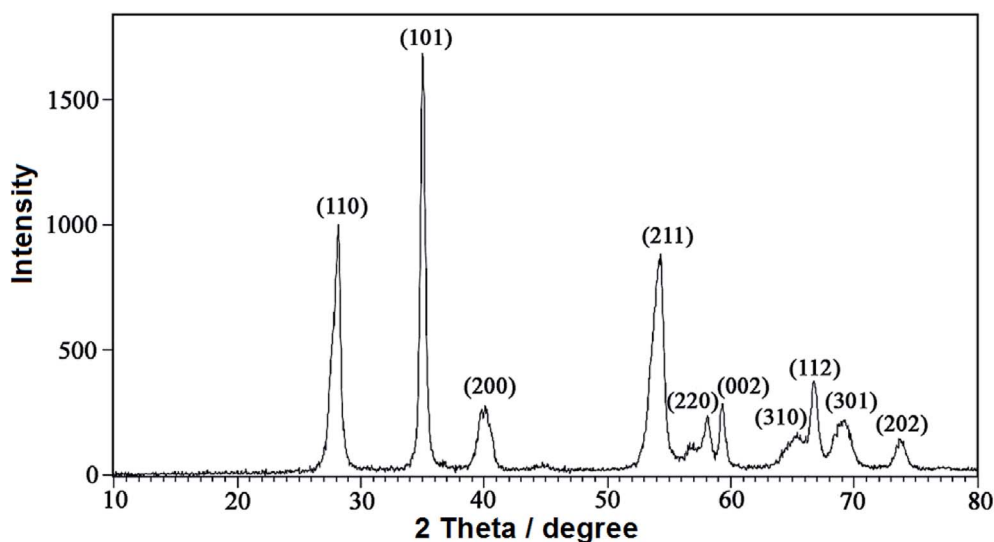


Fig. 4 XRD pattern of RuO₂NPs.

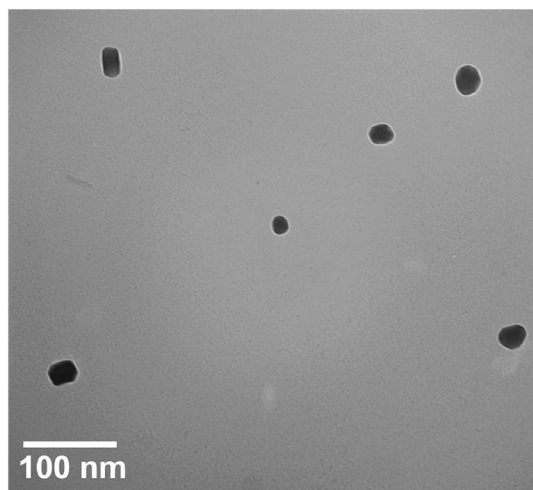


Fig. 5 TEM image of RuO₂NPs.

In addition, we kept the urine specimens inside a refrigerator after being collected. Then, 10 mL of the specimens were centrifuged at 2000 rpm for 15 min. In the next stage, we filtered the supernatant through a 0.45 μm filter. Afterward, different contents of the solution were transferred into a 10 mL volumetric flask, and the solution was diluted to the mark with PBS (pH 7.0). No peak current was observed for clozapine in the urine samples. Then, diverse amounts of clozapine were used to spike the diluted urine specimens. Finally, clozapine contents were examined by our technique *via* the standard addition procedure.

In all two samples, an aliquot of 10 mL of the test solution was placed in the electrochemical cell. The potentials for differential pulse voltammetry (DPV) were controlled between 0.1 and 0.5 V at the scan rate of 50 mV s^{-1} . Anodic peak current (I_{pa}) was measured at the oxidation potential of clozapine.

Results and discussion

RuO₂NP characterization

Fig. 1 displays the scanning electron microscopy (SEM) images of RuO₂NPs. The well-arranged NRs further facilitate the contact of samples with the solution.

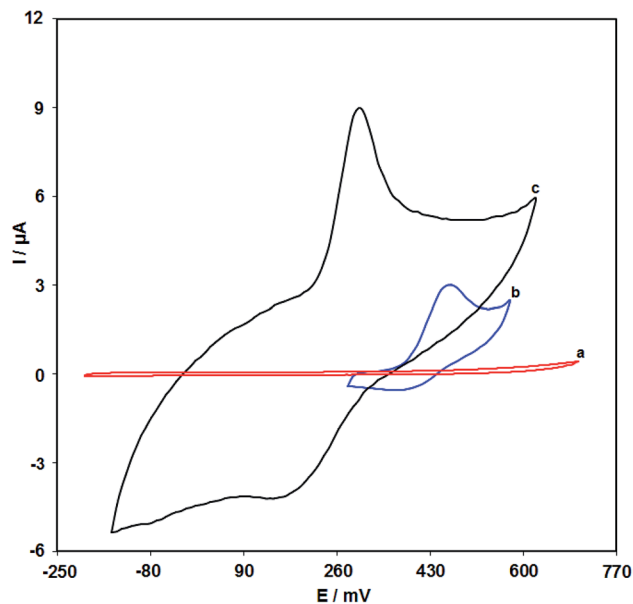


Fig. 7 The cyclic voltammogram of (a) bare SPE in 0.1 M PBS (pH = 7.0) in the absence of clozapine (b) bare SPE and (c) RuO₂ NP/SPE in 0.1 M PBS (pH = 7.0) in the presence of 100.0 μM clozapine at a scan rate of 50 mV s^{-1} .

The energy dispersive X-ray analysis (EDX) of RuO₂ NPs was performed to qualitatively examine the presence of elements and chemical composition of the as-synthesized RuO₂ NPs. As seen in Fig. 2, the EDX spectrum reveals the presence of elemental Ru and O, which approves the higher purity of RuO₂ NPs without obvious impurities.

The EDX elemental mapping analysis was performed for RuO₂ NPs to check the distribution of elements present in the as-synthesized RuO₂ NPs (Fig. 3). Thus, there are O and Ru elements in the as-synthesized RuO₂ NPs.

Fig. 4 shows the X-ray diffraction (XRD) patterns of the RuO₂-NPs synthesized in the present study. In addition, the presence of the miller indices of (110), (101), (200), (211), (220), (002), (310), (112), (301) and (202) in the 2θ range of 28.2, 35.1, 39.7, 54.4, 58.1, 59.4, 65.3, 66.8, 69.1 and 73.8 degree, respectively, confirmed the

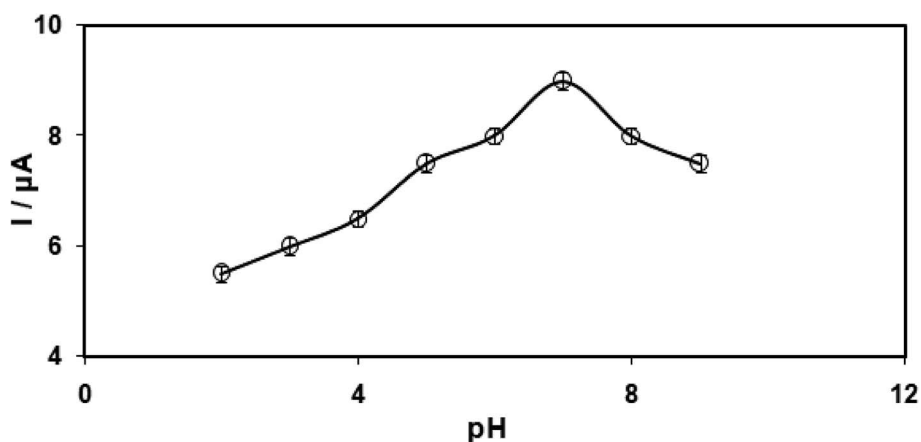


Fig. 6 Plot of I_{pa} vs. pH of 0.1 M PBS (2.0, 3.0, 4.0, 5.0, 6.0, 7.0, 8.0, and 9.0) at the surface of RuO₂ NPs/SPE with 100.0 μM clozapine.



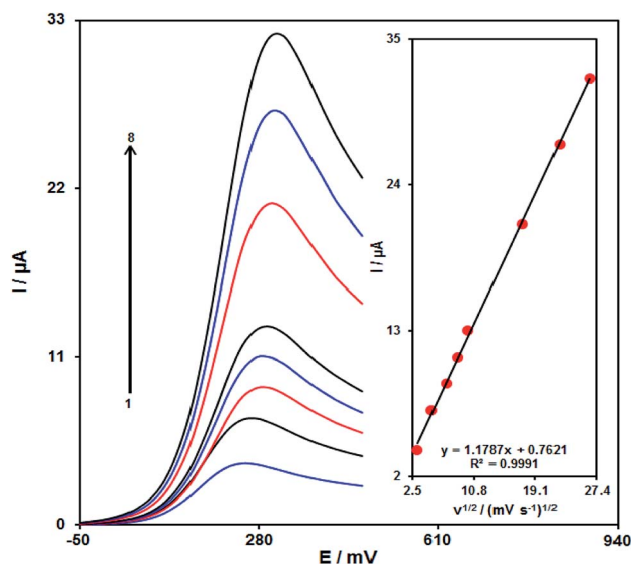


Fig. 8 Linear sweep voltammogram of RuO₂ NP/SPE in 0.1 M PBS (pH = 7.0) consisting of 100.0 μM clozapine at different scan rates. Numbering 1–8 refer to 10, 25, 50, 75, 100, 300, 500, and 700 mV s⁻¹. Inset shows the variation of anodic peak current vs. $v^{1/2}$.

tetragonal structure for RuO₂ NPs (JCPDS 21-1172). The average size of RuO₂NPs is calculated using the Scherrer's equation:⁴⁷

$$d = k\lambda/\beta \cos \theta \quad (1)$$

where d is the size of NPs; k is the Scherrer's constant; λ is the X-ray wavelength; β is the width of the XRD peak at half height; and θ is the Bragg diffraction angle in degree. The average size of RuO₂NPs is calculated to be 35.74 nm.

Fig. 5 displays the transmission electron microscopy (TEM) image of RuO₂NPs. The NPs have an average size of ~20 nm.

Electrochemical behaviour of clozapine on the RuO₂ NP/SPE

It is crucial to have an optimal pH-value for studying the electrochemical behaviour of clozapine that is pH-dependent so that we can reach precise outputs. However, we conducted the tests by employing the modified electrodes at distinct pH-values in the range between 2.0 and 9.0 in 0.1 M phosphate buffer saline (PBS). The results indicated the occurrence of the most acceptable outputs for clozapine electro-oxidation at pH equal to 7.0 (Fig. 6).

Fig. 7 shows the cyclic voltammograms in the presence of 100.0 μM clozapine through the bare SPE (curve b) and the RuO₂ NP/SPE

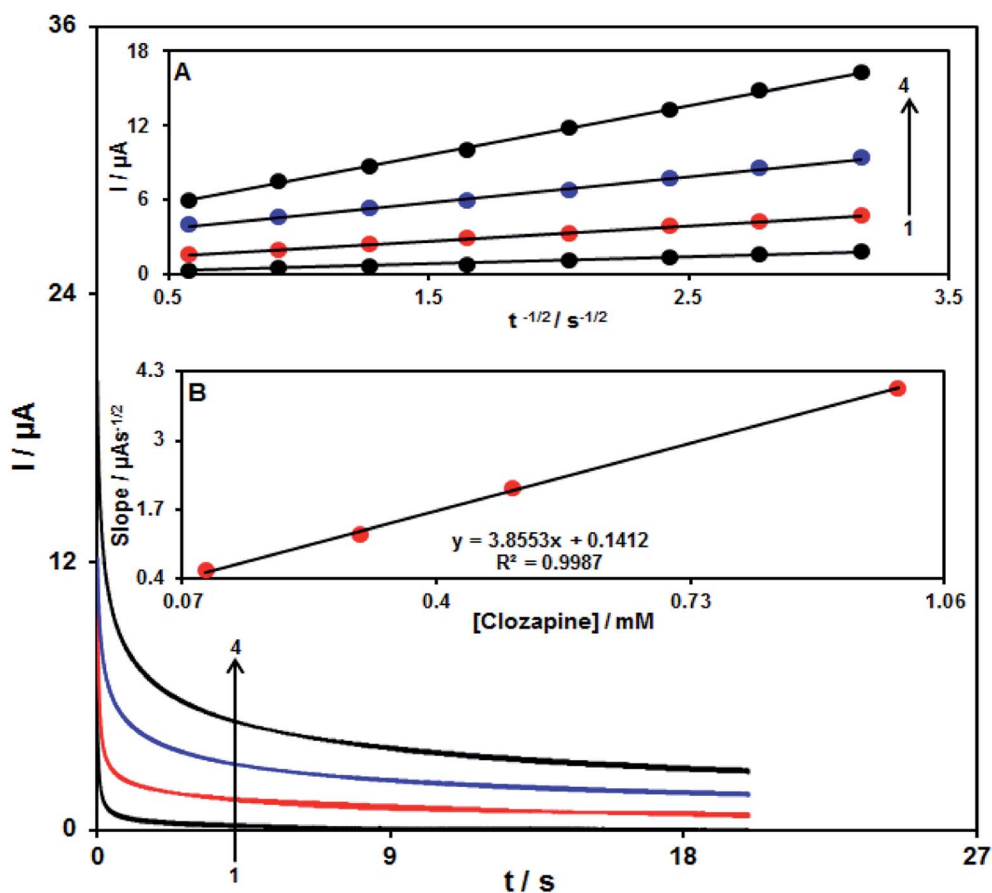


Fig. 9 Chronoamperograms achieved at the RuO₂ NP/SPE in 0.1 M PBS (pH = 7.0) for the different concentrations of clozapine. Numbering 1–4 refer to the 0.1, 0.3, 0.5 and 1.0 mM concentrations of clozapine. Insets: (A) I / plot vs. $t^{-1/2}$ achieved from chronoamperograms 1 to 4. (B) The slope plot of straight lines vs. clozapine concentration.

(curve c). As seen from the CV results, the greatest level of clozapine oxidation on the RuO₂ NP/SPE occurs at 300 mV that is nearly 170 mV more negative in comparison to the unmodified SPE evidencing the reduced polarization owing to the improved conductivity. In addition, CV of the RuO₂ NP/SPE in the absence of clozapine shows no peak current (curve a) suggesting the negligible redox activity. Furthermore, there was an increase in the anodic peak current of clozapine at the surface of the RuO₂ NP/SPE (curve c) compared with that at bare SPE (curve b) because of the existence of RuO₂ NPs at the surface of the electrode, resulting in a higher surface area and electrical conductivity.

Effects of the scan rate on the outputs

It is notable that the increase in the scan rate causes greater oxidation peak currents with regard to outputs gained by examining the effects of potential scan rates on the clozapine oxidation current (Fig. 8). In addition, we found a linear association between I_{pa} and the square root of the potential scan rate ($\nu^{1/2}$), indicating that diffusion controls the clozapine oxidation process.⁴⁸

Chronoamperometric analysis

The chronoamperometry analysis for clozapine samples was conducted using the RuO₂ NP/SPE at 0.35 V. Fig. 9 shows the

chronoamperometric results of different concentrations of clozapine samples in PBS (pH = 7.0). Herein, the Cottrell equation for the chronoamperometry analysis of the electro-active moiety under the mass transfer-limited condition is:⁴⁸

$$I = nFAD^{1/2}C_b\pi^{-1/2}t^{-1/2} \quad (2)$$

where D refers to the diffusion coefficient (cm² s⁻¹). C_b is the applied bulk concentration (mol cm⁻³). Fig. 7a depicts the experimental outputs of I vs. $t^{-1/2}$ so that the best fit has been obtained for the different concentrations of clozapine. Moreover, Fig. 7b shows the resultant slopes relative to the straight line in Fig. 7a vs. the clozapine concentration. In addition, the mean value of D was calculated to be 1.3×10^{-6} cm² s⁻¹ based on the Cottrell equation and the final slope of Fig. 7b. This value is comparable with the diffusion coefficient value obtained in a previous research (2.1×10^{-5} cm² s⁻¹).⁴⁹

Calibration curve

With regard to the clozapine resultant peak currents at the RuO₂ NP/SPE, clozapine was quantitatively analysed in water (Fig. 10). We also utilized the modified electrode (RuO₂ NP/SPE) as the working electrode within a range of clozapine. DPV, because of its greater sensitivity and more reasonable functions in the

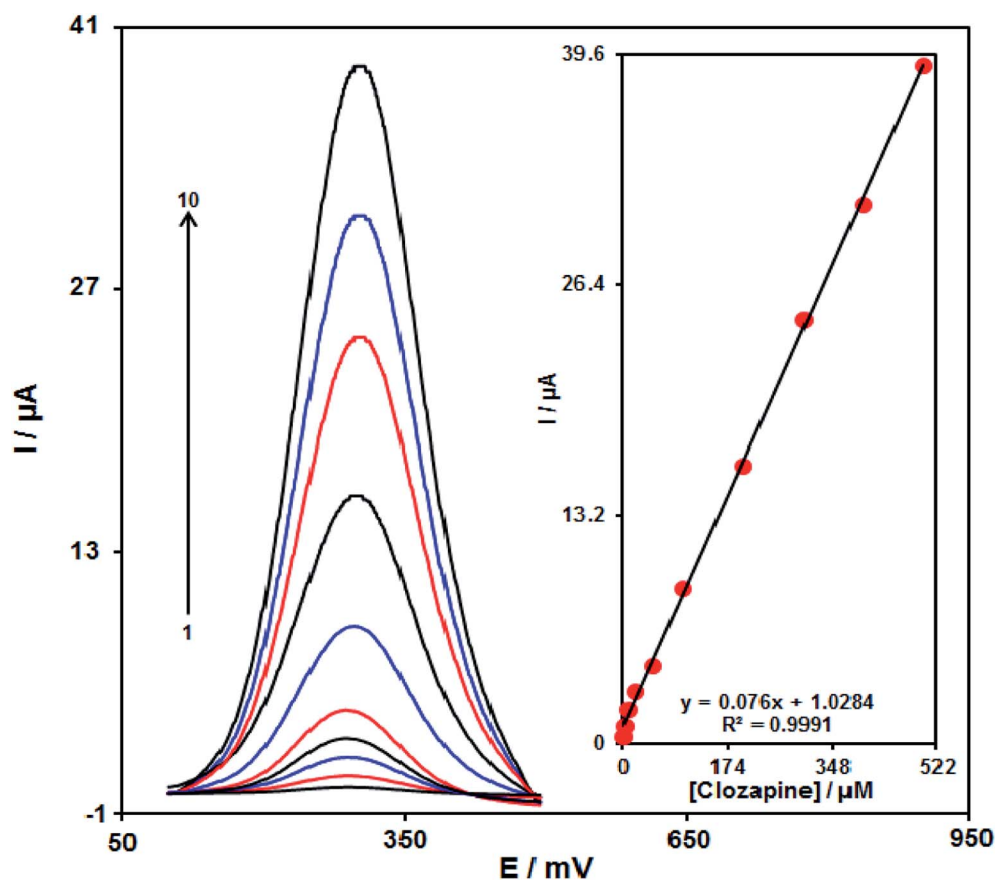


Fig. 10 Differential pulse voltammograms of the RuO₂ NP/SPE in the 0.1 M PBS (pH = 7.0) consisting of different concentrations of clozapine. Numbering 1–10 refer to 0.2, 2.5, 7.5, 20.0, 50.0, 100.0, 200.0, 300.0, 400.0, and 500.0 μM of clozapine. Inset: the peak current plot as a function of clozapine concentration ranging between 0.1 and 500.0 μM.



Table 1 The application of the RuO₂ NP/SPE for the determination of clozapine in real samples ($n = 5$). All concentrations are in μM

Sample	Spiked	Found	Recovery (%)	R.S.D. (%)
Clozapine tablet	0	4.5	—	0.2
	2.5	5.9	98.3	1.7
	7.5	12.4	103.3	2.8
	12.5	17.2	101.2	2.4
	17.5	21.8	99.1	1.9
Urine	0	—	—	—
	5.0	4.9	98.0	1.9
	10.0	10.1	101	2.3
	15.0	14.9	99.3	2.2
	20.0	20.6	103.0	3.5

analytical utilizations, was used with the following parameters: initial potential (0.1 V), end potential (0.5 V), step potential (10 mV) and modulation amplitude (25 mV). However, outputs implied the linear relationship between peak currents and clozapine concentrations in the concentration range between 0.2 and 500.0 μM , having a correlation coefficient of 0.9991 and a sensitivity of 0.076 $\mu\text{A} \cdot \mu\text{M}^{-1}$. Finally, the detection limit at 3σ was determined to be 0.07 μM .

Reproducibility and stability of the RuO₂ NP/SPE

In order to test the RuO₂ NP/SPE stability, we maintained our sensor at pH 7.0 in PBS for 14 days and recorded the cyclic voltammograms of the solution consisting of 30.0 μM of clozapine in order to compare to the cyclic voltammogram achieved prior to the immersion. Results show no change in the clozapine oxidation peak. Moreover, the current declined by approximately 2% in the signals as compared with the initial responses, implying a reasonable stability of the RuO₂ NP/SPE.

We analyzed the antifouling feature of the modified SPE toward clozapine oxidation and its products *via* CV for the modified SPE prior to and following its utilization in the presence of clozapine. Moreover, we recorded cyclic voltammogram in the presence of clozapine following the cycling of the potential fifteen times at a 50 mV s⁻¹. Results showed decline in the currents by approximately 2% and no alteration in the peak potentials.

Analysis of real samples

We used clozapine in the clozapine tablet and the urine samples *via* the aforementioned procedure in order to assess the proposed modified electrode utility to detect the real samples. Therefore, a standard addition procedure was utilized. Table 1 reports the analysis outputs. The test outcomes showed acceptable recoveries for clozapine. The method reproducibility was investigated *via* the relative standard deviation (RSD).

Conclusions

The present study measured the detection of clozapine at a RuO₂ NP/SPE. According to the results, RuO₂ NPs have stability, higher responses, and sensitive detection towards

clozapine in comparison with the unmodified SPE. The RuO₂ NP/SPE has higher electro-catalytic activities toward clozapine oxidation, indicating 0.076 $\mu\text{A} \cdot \mu\text{M}^{-1}$ sensitivity, a low detection limit of 0.07 μM , and a large linear range of response with the clozapine concentration of 0.2 to 500.0 μM . At the end, this technique ability has been shown in the detection of clozapine in the real specimens with reasonable outputs. Therefore, the RuO₂ NP/SPE showed the potential of being constructed as an electrochemical sensor to detect clozapine quantitatively.

Conflicts of interest

There are no conflicts to declare.

Acknowledgements

The authors acknowledge the financial support provided for this project (Project No. 98000791) by Neuroscience Research Center, Kerman University of Medical Sciences, Kerman, Iran. Also, this research was supported by the Future Material Discovery Program (2016M3D1A1027666), Basic Science Research Program (2017R1A2B3009135) through the National Research Foundation of Korea. Also, China Scholarship Council (201808260042) is appreciated.

References

- C. J. Carter, *Schizophr. Res.*, 2006, **86**, 1–14.
- S. Ulrich, R. Wolf and J. Staedt, Serum level of clozapine and relapse, *Ther. Drug Monit.*, 2003, **25**, 252–255.
- A. A. Mohamed and S. M. Al-Ghannam, *Farmaco*, 2004, **59**, 907–911.
- W. Jin, Q. Xu and W. Li, *Electrophoresis*, 2000, **21**, 1415–1420.
- M. M. Zheng, S. T. Wang, W. K. Hu and Y. Q. Feng, *J. Chromatogr. A*, 2010, **1217**, 7493–7501.
- I. Vardakou, A. Dona, C. Pistos, G. Alevisopoulos, S. Athanaselis, C. Maravelias and C. Spiliopoulou, *J. Chromatogr. B: Anal. Technol. Biomed. Life Sci.*, 2010, **878**, 2327–2332.
- G. Zhang, A. V. Terry Jr and M. G. Bartlett, *J. Chromatogr. B: Anal. Technol. Biomed. Life Sci.*, 2007, **856**, 20–28.
- A. Wohlfarth, N. Toepfner, M. Hermanns-Clausen and V. Auwärter, *Anal. Bioanal. Chem.*, 2011, **400**, 737–746.
- K. Farhadi and A. Karimpour, *Anal. Sci.*, 2007, **23**, 479–483.
- M. Arvand and M. G. Shiraz, *Electroanalysis*, 2012, **24**, 683–690.
- A. Shamsi, F. Ahour and B. Sehatnia, *J. Solid State Electrochem.*, 2018, **22**, 2681–2689.
- M. Mazloum-Ardakani, H. Beitollahi, M. K. Amini, F. Mirkhalaf, B. F. Mirjalili and A. Akbari, *Analyst*, 2011, **136**, 1965–1970.
- K. Zhang, T. H. Lee, M. A. Khalilzadeh, R. S. Varma, J.-W. Choi, H. W. Jang and M. Shokouhimehr, *ACS Omega*, 2020, **5**, 1634–1639.
- K. Zhang, T. H. Lee, J. H. Cha, R. S. Varma, J.-W. Choi, H. W. Jang and M. Shokouhimehr, *ACS Omega*, 2019, **4**, 21410–21416.



- 15 K. Zhang, T. H. Lee, J. H. Cha, H. W. Jang, J.-W. Choi, M. Mahmoudi and M. Shokouhimehr, *Sci. Rep.*, 2019, **9**, 1–8.
- 16 K. Zhang, T. H. Lee, H. Noh, T. Islamoglu, O. K. Farha, H. W. Jang, J.-W. Choi and M. Shokouhimehr, *ACS Appl. Mater. Interfaces*, 2019, **11**, 31799–31805.
- 17 K. Zhang, T. H. Lee, B. Bubach, M. Ostadhassan, H. W. Jang, J.-W. Choi and M. Shokouhimehr, *RSC Adv.*, 2019, **9**, 26668–26675.
- 18 K. Zhang, T. H. Lee, B. Bubach, M. Ostadhassan, H. W. Jang, J.-W. Choi and M. Shokouhimehr, *RSC Adv.*, 2019, **9**, 21363–21370.
- 19 P. Nicholas, R. Pittson and J. P. Hart, *Food Chem.*, 2018, **241**, 122–126.
- 20 M. A. Khalilzadeh, S. Tajik, H. Beitollahi and R. A. Venditti, *Ind. Eng. Chem. Res.*, 2020, **59**, 4219–4228.
- 21 S. Srikanta, P. Parmeswaranaik and G. Krishnamurthy, *Asian J. Green Chem.*, 2019, DOI: 10.33945/SAMI/AJGC/2020.2.1.
- 22 P. Bollella, G. Fusco, D. Stevar, L. Gorton, R. Ludwig, S. Ma, H. Boer, A. Koivula, C. Tortolini, G. Favero and R. Antiochia, *Sens. Actuators, B*, 2018, **256**, 921–930.
- 23 M. R. Ganjali, Z. Dourandish, H. Beitollahi, S. Tajik, L. Hajiaghababaei and B. Larijani, *Int. J. Electrochem. Sci.*, 2018, **13**, 2448–2461.
- 24 K. Zhang, T. H. Lee, O. K. Farha, H. W. Jang, J.-W. Choi and M. Shokouhimehr, *Cryst. Growth Des.*, 2019, **19**, 7385–7395.
- 25 M. A. Khalilzadeh and M. Borzoo, *J. Food Drug Anal.*, 2016, **24**, 796–803.
- 26 H. Beitollahi, S. Tajik, M. H. Asadi and P. Biparva, *J. Anal. Sci. Technol.*, 2014, **5**, 1–9.
- 27 K. Zhang, T. H. Lee, M. A. Khalilzadeh, R. S. Varma, J.-W. Choi, H. W. Jang and M. Shokouhimehr, *ACS Omega*, 2020, **5**, 1634–1639.
- 28 K. Zhang, T. H. Lee, J. H. Cha, H. W. Jang, M. Shokouhimehr and J.-W. Choi, *Electron. Mater. Lett.*, 2019, **15**, 727–732.
- 29 H. Beitollahi, M. A. Khalilzadeh, S. Tajik, M. Safaei, K. Zhang, H. W. Jang and M. Shokouhimehr, *ACS Omega*, 2020, **5**, 2049–2059.
- 30 K. Zhang, T. H. Lee, J. H. Cha, H. W. Jang, M. Shokouhimehr and J.-W. Choi, *Electron. Mater. Lett.*, 2019, **15**, 720–726.
- 31 S. Tajik, M. A. Taher, H. Beitollahi and M. Torkzadeh-Mahani, *Talanta*, 2015, **134**, 60–64.
- 32 K. Zhang, R. S. Varma, H. W. Jang, J.-W. Choi and M. Shokouhimehr, *J. Alloys Compd.*, 2019, **791**, 911–917.
- 33 K. Zhang, T. H. Lee, J. H. Cha, R. S. Varma, J.-W. Choi, H. W. Jang and M. Shokouhimehr, *Sci. Rep.*, 2019, **9**, 1–10.
- 34 S. Esfandiari-Baghbamidi, H. Beitollahi, S. Tajik and R. Hosseinzadeh, *Int. J. Electrochem. Sci.*, 2016, **11**, 10874–10883.
- 35 N. Rabiee, M. Safarkhani and M. Rabiee, *Asian J. Nanosci. Mater.*, 2018, **1**, 63–73.
- 36 Y. Li, X. Zhai, X. Liu, L. Wang, H. Liu and H. Wang, *Talanta*, 2016, **148**, 362–369.
- 37 M. A. Khalilzadeh and Z. Arab, *Curr. Anal. Chem.*, 2017, **13**, 81–86.
- 38 H. Beitollahi, H. Karimi-Maleh and H. Khabazzadeh, *Anal. Chem.*, 2008, **80**, 9848–9851.
- 39 D. W. Li, Y. T. Li, W. Song and Y. T. Long, *Anal. Methods*, 2010, **2**, 837–843.
- 40 Z. Shamsadin-Azad, M. A. Taher, S. Cheraghi and H. Karimi-Maleh, *J. Food Meas. Charact.*, 2019, **13**, 1781–1787.
- 41 C. Karuppiyah, K. Muthupandi, S. M. Chen, M. A. Ali, S. Palanisamy, A. Rajan, P. Prakash, F. M. A. Al-Hemaid and B. S. Lou, *RSC Adv.*, 2015, **5**, 31139–31146.
- 42 S. Tajik, H. Beitollahi and P. Biparva, *J. Serb. Chem. Soc.*, 2018, **83**, 863–874.
- 43 W. H. Elobeid and A. A. Elbashir, *Prog. Chem. Biochem. Res.*, 2019, **2**, 24–33.
- 44 Y. Yang, A. M. Asiri, D. Du and Y. Lin, *Analyst*, 2014, **139**, 3055–3060.
- 45 N. Soin, S. S. Roy, S. K. Mitra, T. Thundat and J. A. McLaughlin, *J. Mater. Chem.*, 2012, **22**, 14944–14950.
- 46 M. D. Stoller, S. Park, Y. Zhu, J. An and R. S. Ruoff, *Nano Lett.*, 2008, **8**, 3498–3502.
- 47 S. Tajik, H. Mahmoudi-Moghaddam and H. Beitollahi, *J. Electrochem. Soc.*, 2019, **166**, B402–B406.
- 48 A. J. Bard and L. R. Faulkner, *Electrochemical methods fundamentals and applications*, Wiley, New York, 2nd edn, 2001.
- 49 F. Huang, S. Qu, S. Zhang, B. Liu and J. Kong, *Talanta*, 2007, **72**, 457–462.

